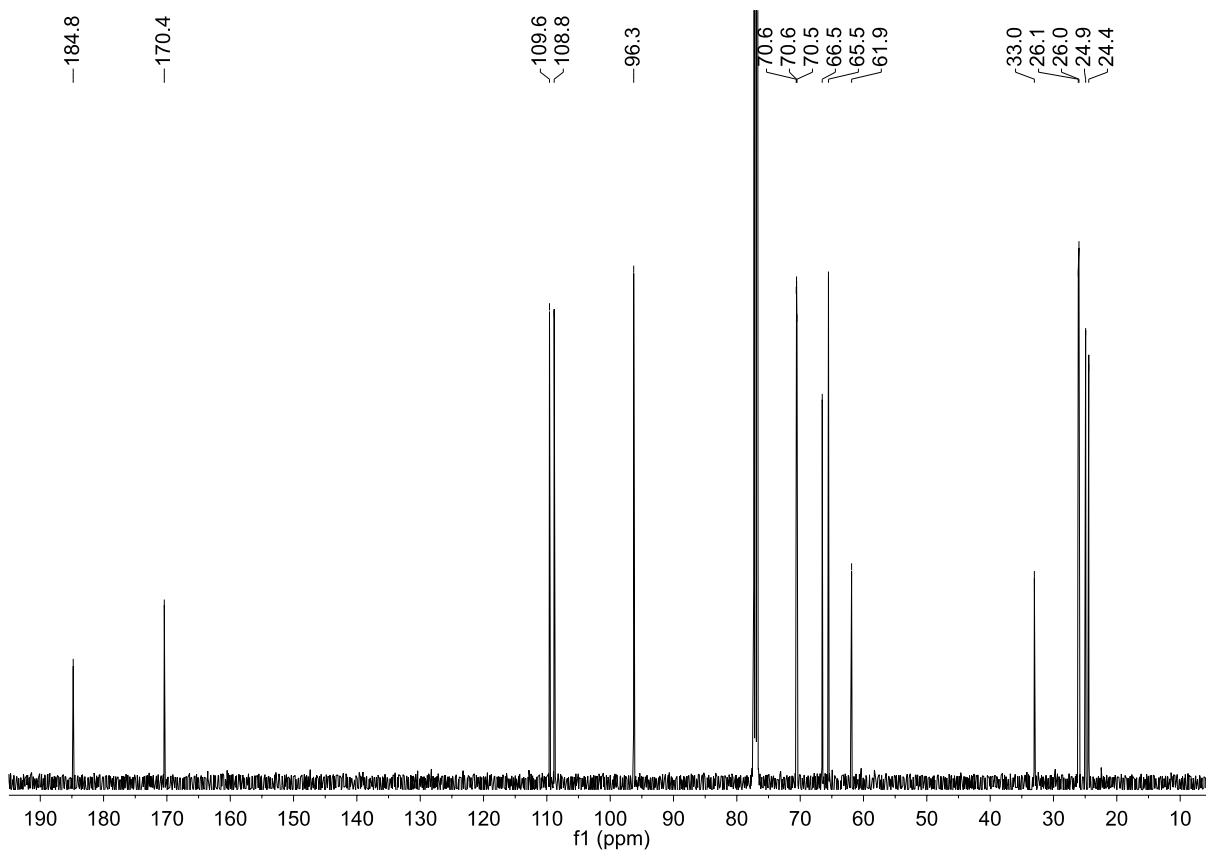
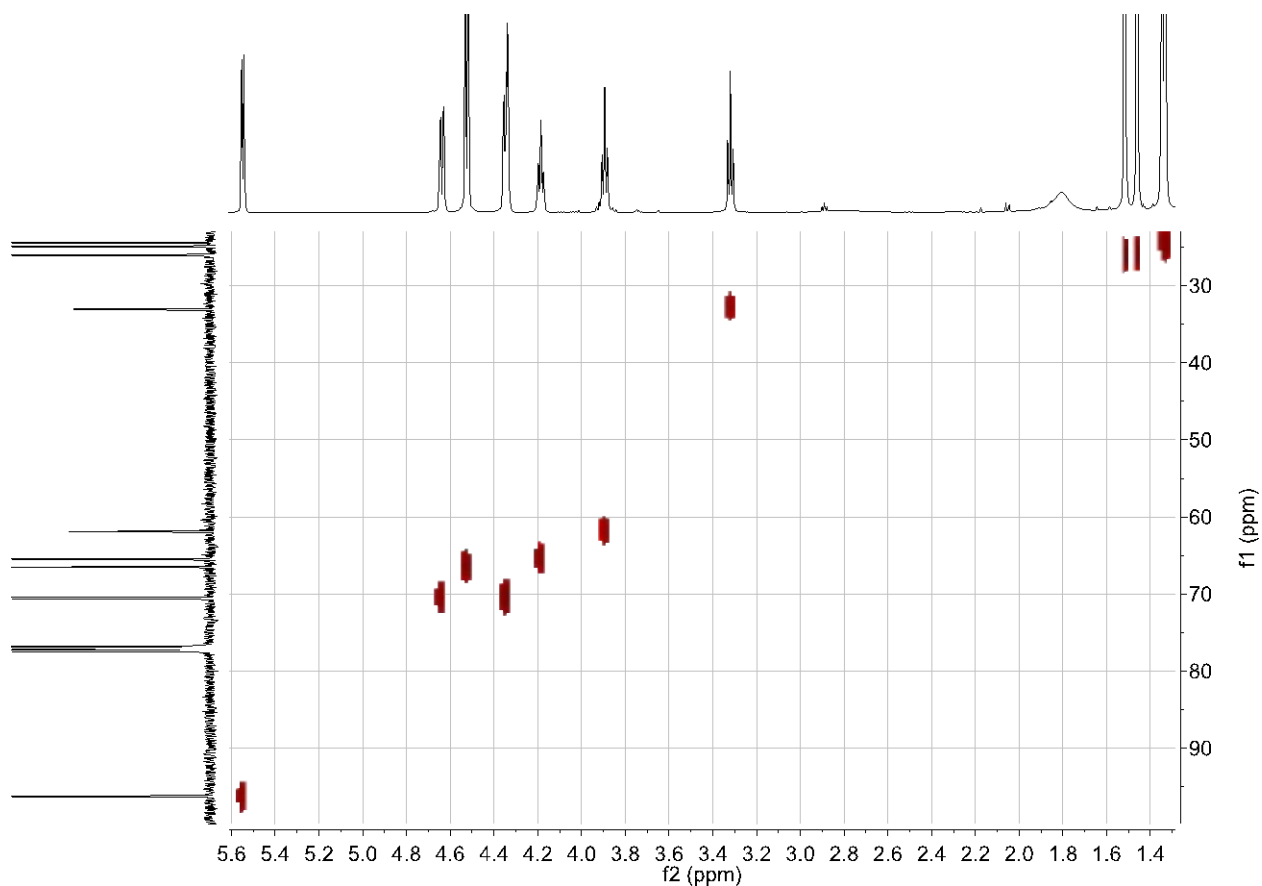


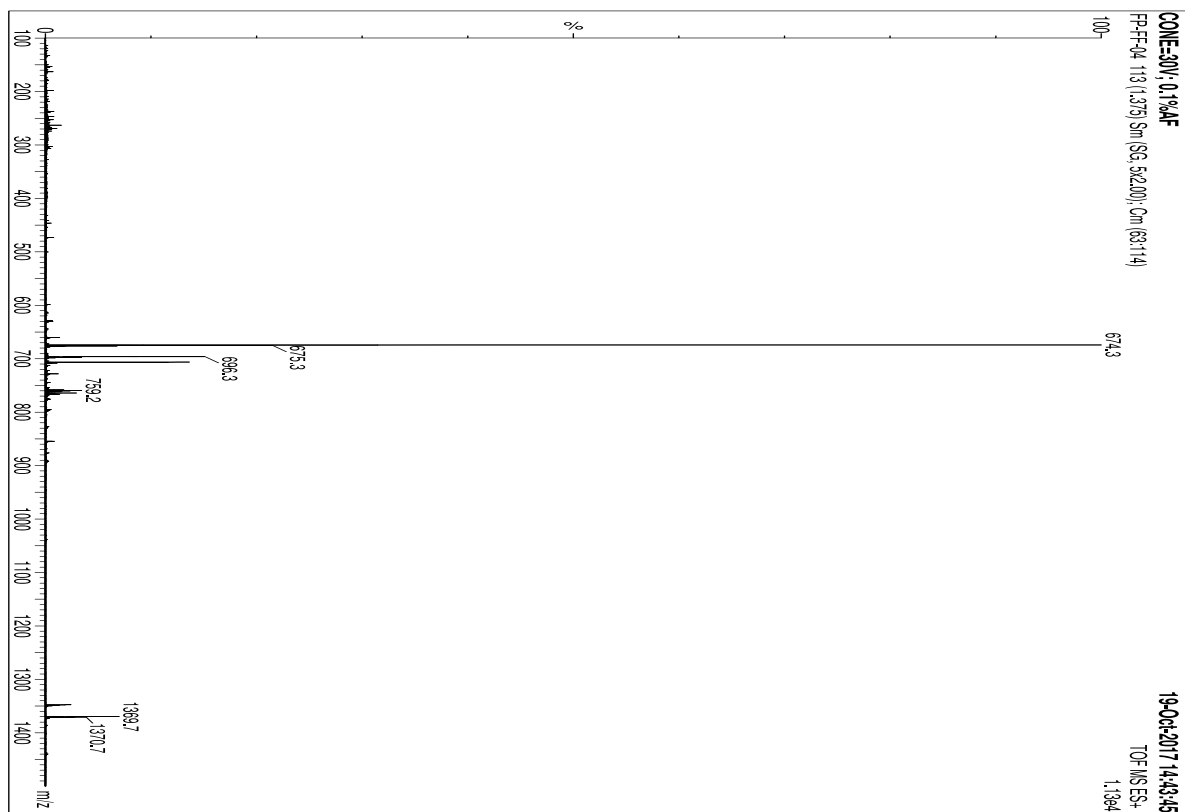
**Supplemental Figure 1.**  $^1\text{H}$  NMR spectra of compound **1**. Compound **1** was dissolved in chloroform-*d* and  $^1\text{H}$  NMR spectra acquired at 500 MHz. The full interpretation of the data is in the results section of the manuscript.



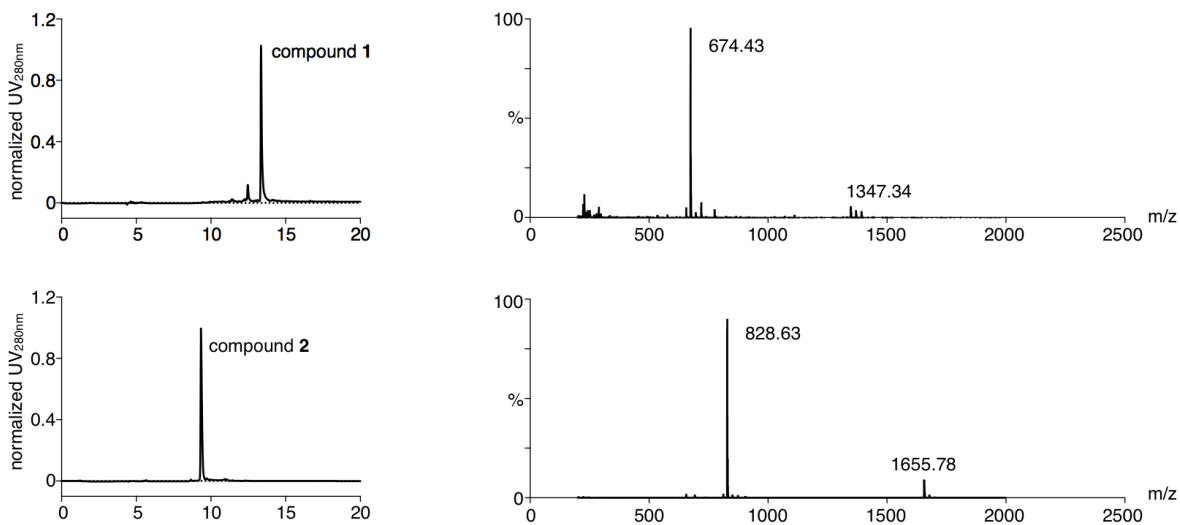
**Supplemental Figure 2.**  $^{13}\text{C}$  NMR spectra of compound **1**. Compound **1** was dissolved in chloroform-*d* and  $^1\text{H}$  NMR spectra acquired at 500 MHz. The full interpretation of the data is in the results section of the manuscript.



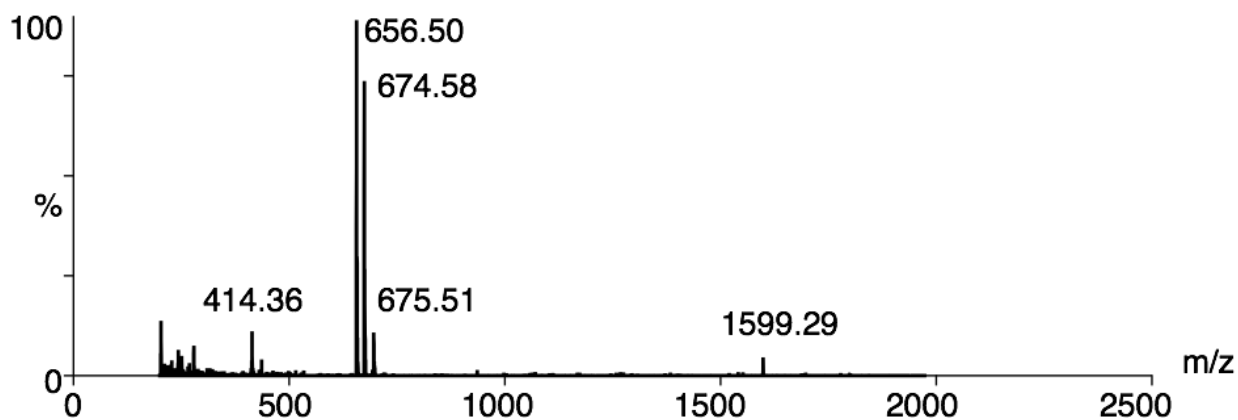
**Supplemental Figure 3.** Heteronuclear Single Quantum Coherence (HSQC) spectra of compound **1** to determine proton-carbon single bond correlations. Protons lie along the observed x-axis and carbons lie along the observed y-axis. Full interpretations of the data allowed for the full C-H structure determination of the compound reported in the results section of the manuscript.



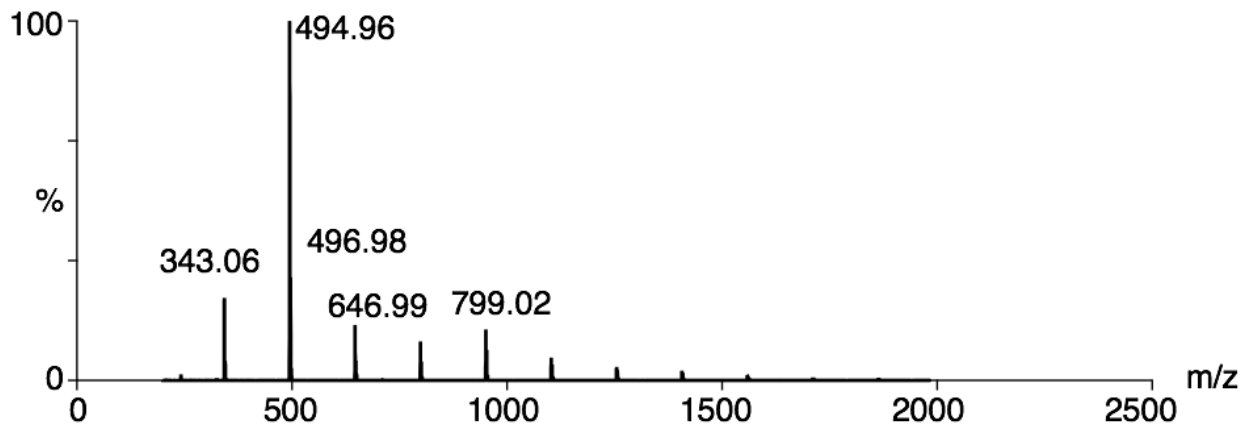
**Supplemental Figure 4.** Electrospray ionization mass spectrometry (ESI-MS) spectra of compound **1**. Calculated mass to charge ratio ( $m/z$ ) for compound **1** was 673.25 and mass found was 674.3  $[M + H]^+$ .



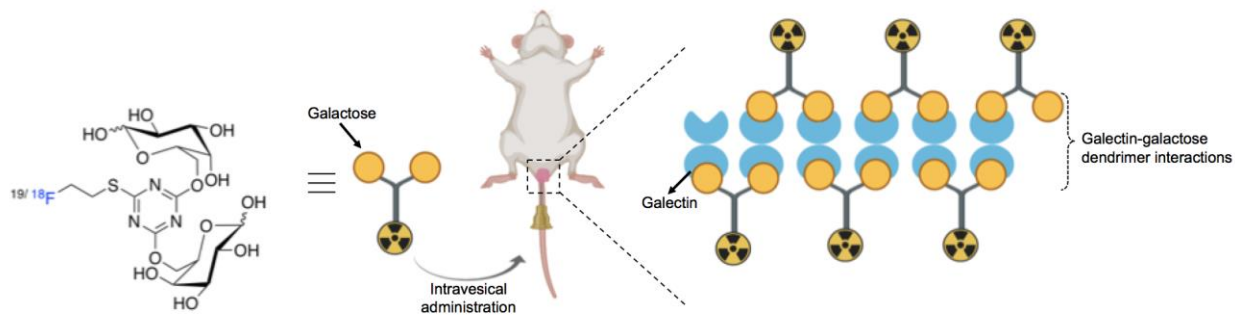
**Supplemental Figure 5.** HPLC chromatogram (*left*) ESI-MS spectra (*right*) of compound **1** and compound **2**. Calculated mass to charge ratio ( $m/z$ ) for compound **2** was 827.26 and mass found 828.63  $[M + H]^+$ .



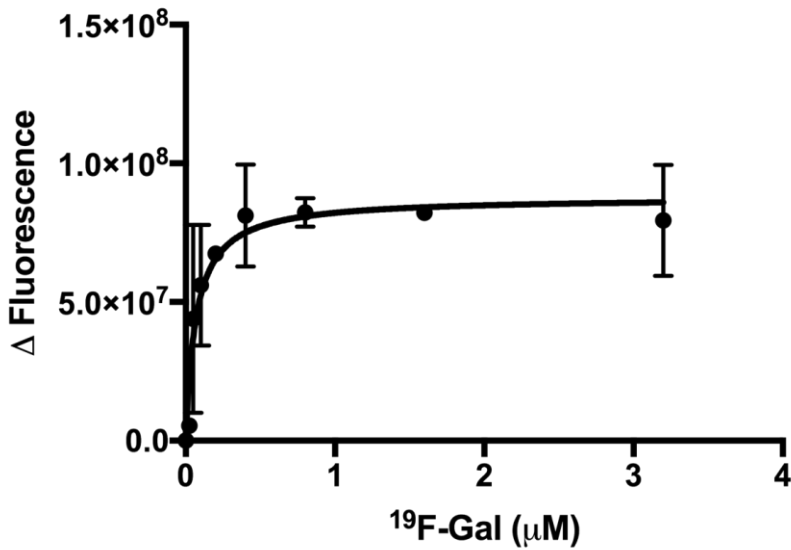
**Supplemental Figure 6.** ESI-MS spectra of compound **3**. Calculated mass to charge ratio ( $m/z$ ) for compound **3** was 656.25 and mass found 656.50  $[M + H]^+$ .



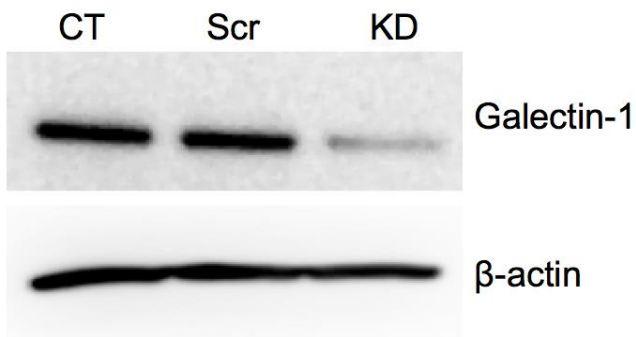
**Supplemental Figure 7.** ESI-MS spectra of compound 4. Calculated mass to charge ratio ( $m/z$ ) for compound 3 was 496.12 and mass found 496.98  $[M + H]^+$ .



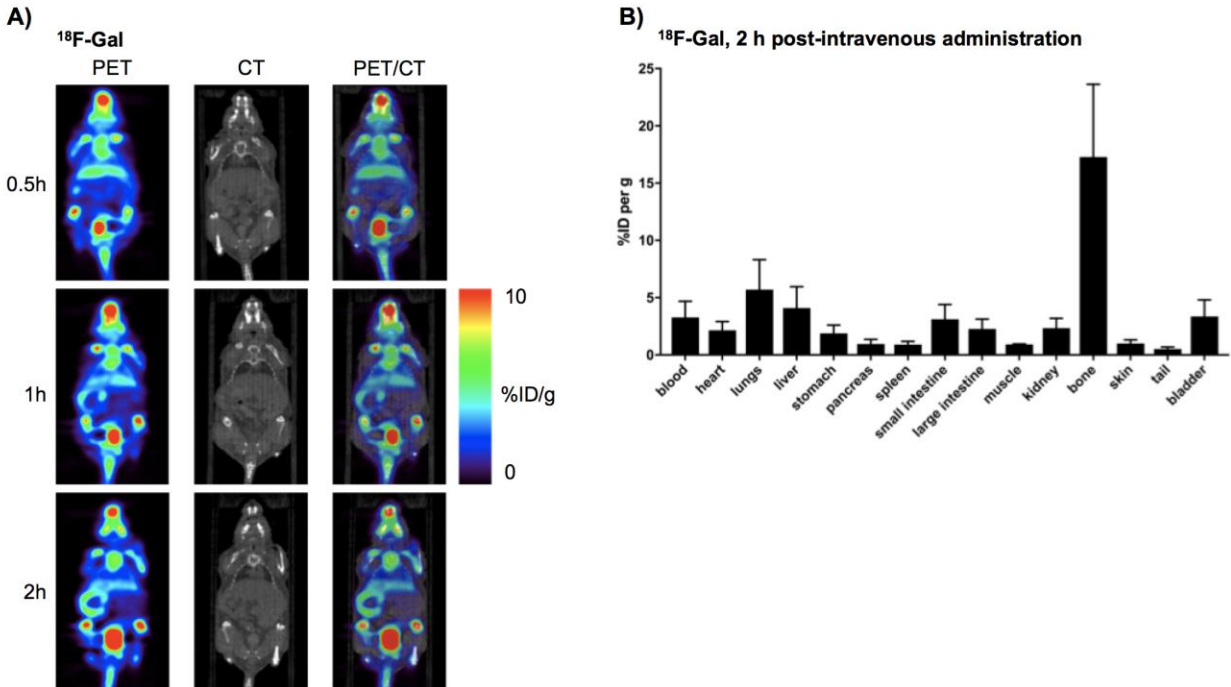
**Supplemental Figure 8.** The F-18 containing galactodendritic unit 4 was administered via intravesical injections into the bladder of mice bearing orthotopic UMUC3 bladder cancer cells. The galactose dendritic moieties in  $^{18}\text{F}$ -labeled galactodendritic unit 4 interact with galectin-1 at the tumor cells, allowing BCa PET imaging.



**Supplemental Figure 9.** Fluorescence variation on the emission spectrum of 2  $\mu\text{M}$  galectin-1 protein after the addition of [ $^{19}\text{F}$ ]compound 4. Data are means  $\pm$  S.E.M. of three independent experiments.

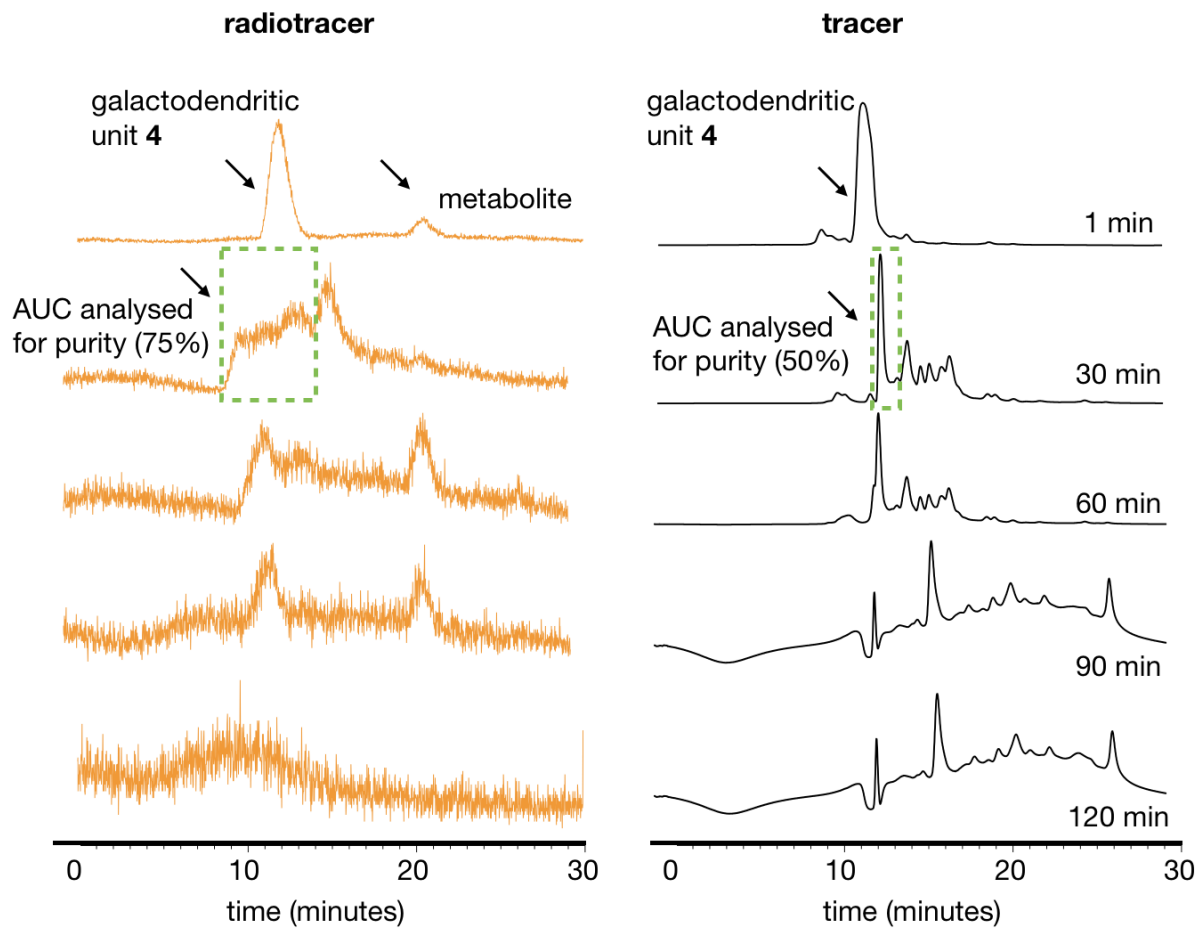


**Supplemental Figure 10.** Western blot analysis of galectin-1 in the total lysates of UMUC3 before and after knockdown using siRNA. Scr, scrambled siRNA.

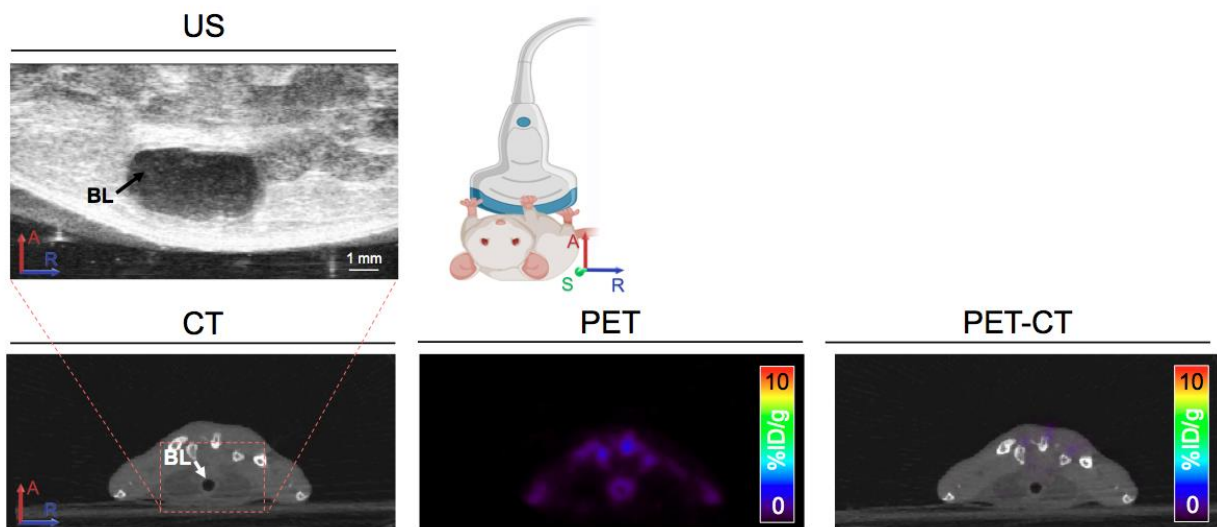


**Supplemental Figure 11.** (A) Representative coronal PET images and (B) biodistribution data of  $^{18}\text{F}$ -labeled galactodendritic unit 4 in athymic nude mice bearing orthotopic UMUC3 bladder tumors. Mice were intravenous administrated  $^{18}\text{F}$ -labeled galactodendritic unit 4 (2.9 – 3.3 MBq) and PET/CT images acquired at 0.5, 1, and 2 h post-administration of the galactose radiotracer. Biodistribution was performed at 2 h post-injection of  $^{18}\text{F}$ -labeled galactodendritic unit 4 (Bars,  $n = 4$  mice per group, mean  $\pm$  S.E.M). CT, Computer Tomography; PET, Positron Emission Tomography; %ID/g, percentage of injected dose per gram of tissue.

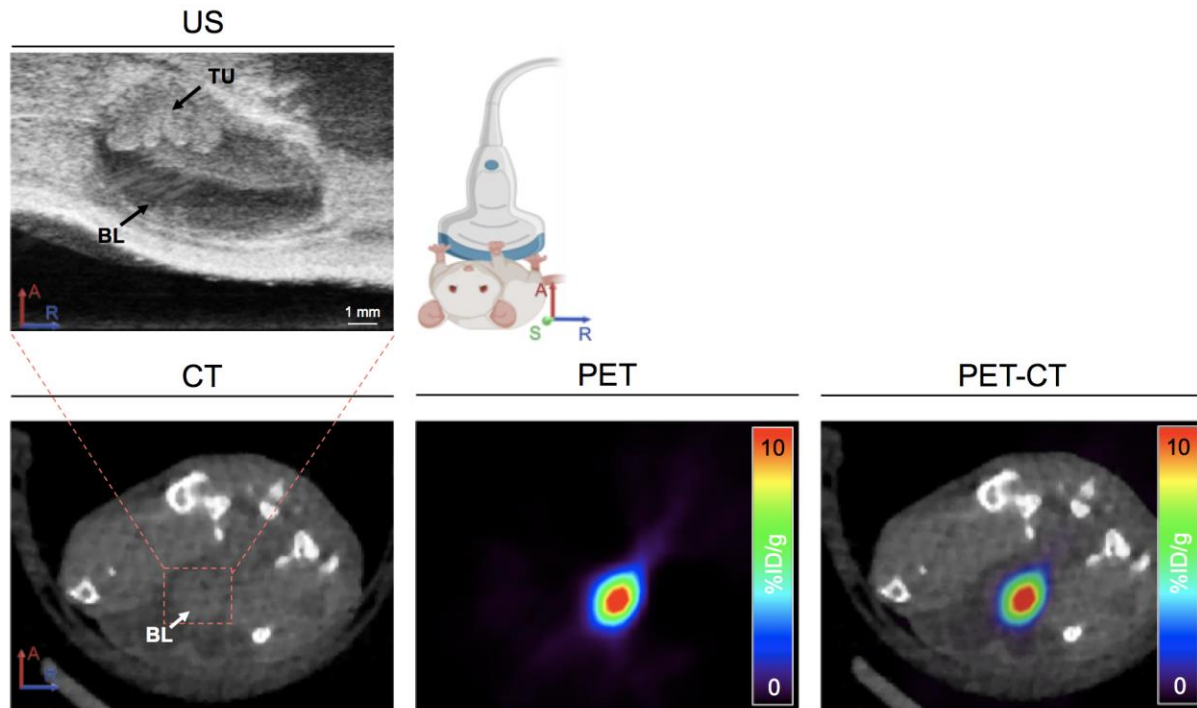




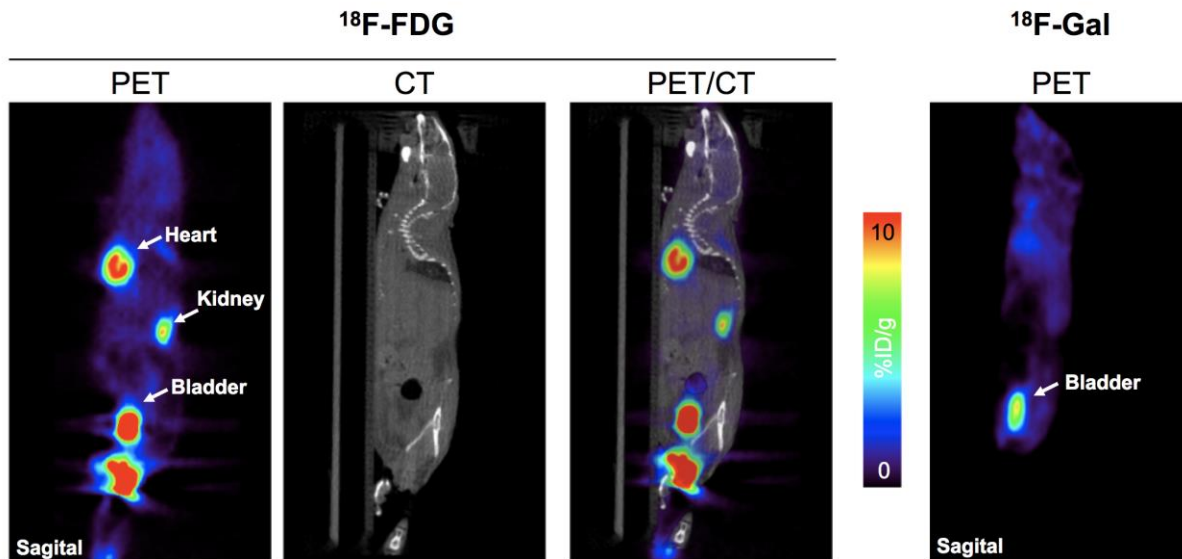
**Supplemental Figure 12.** Stability of  $^{18}\text{F}$ -labeled galactodendritic unit **4** in saline sample containing 10.5% (v/v) mice urine. **(left)** Radiotracer chromatogram of  $^{18}\text{F}$ -labeled galactodendritic unit **4** in a saline sample containing mice urine at various time-points post-incubation (1 min, 30 min, 60 min, 90 min, and 120 min). **(right)** Corresponding HPLC chromatogram (280 nm) of  $^{18}\text{F}$ -labeled galactodendritic unit **4** in a saline sample containing mice urine at various time-points post-incubation (1 min, 30 min, 60 min, 90 min, and 120 min). AUC, area under the curve.



**Supplemental Figure 13. Top panel**, Ultrasound image of murine bladders of non-tumor bearing mice. **Lower panel**, Representative axial PET images at 1 h after administration of  $^{18}\text{F}$ -labeled galactodendritic unit 4 in athymic nude mice. Mice were intravesical administrated  $^{18}\text{F}$ -labeled galactodendritic unit 4 (14.7 – 15.3 MBq), the bladder was flushed with PBS, and PET/CT images were acquired at 1 h post-administration of the galactose radiotracer. US, ultrasound; BL, bladder; TU, tumor; CT, Computer Tomography; PET, Positron Emission Tomography.



**Supplemental Figure 14.** **Top panel,** Ultrasound images of murine bladders at 15 days after UMUC3 cells' implantation in the bladder. **Lower panel,** Representative axial PET images at 1 h after administration of  $^{18}\text{F}$ -FDG in athymic nude mice bearing orthotopic UMUC3 bladder tumors. Mice were intravesical administrated  $^{18}\text{F}$ -FDG (14.7 – 15.3 MBq), the bladder flushed with PBS, and PET/CT images acquired at 1 h post-administration of the glucose radiotracer. US, ultrasound; BL, bladder; TU, tumor; CT, Computer Tomography; PET, Positron Emission Tomography.



**Supplemental Figure 15.** Representative sagittal PET images of **(left)**  $^{18}\text{F}$ -FDG and **(right)**  $^{18}\text{F}$ -labeled galactodendritic unit 4 in athymic nude mice bearing orthotopic UMUC3 bladder tumors. Mice were intravesical administrated  $^{18}\text{F}$ -FDG or  $^{18}\text{F}$ -labeled galactodendritic unit 4 (14.7 – 15.3 MBq), the bladder was flushed with PBS, and PET/CT images were acquired at 1 h post-administration of the glucose or galactose radiotracer. CT, Computer Tomography; PET, Positron Emission Tomography.